Anal. Chem. **1997,** *69,* 4680−4687

Spatially Resolved Raman Spectroscopy of Carbon Electrode Surfaces: Observations of Structural and Chemical Heterogeneity

Kenneth Ray, III and Richard L. McCreery*

Department of Chemistry, The Ohio State University, 100 West 18th Avenue Columbus, Ohio, 43210

Raman spectroscopy and Raman imaging were used to examine several types of carbon electrode materials, including glassy carbon (GC) and highly ordered pyrolytic graphite (HOPG). Variations in the intensity ratio of the D and E_{2g} Raman bands across the carbon surface indicated varying carbon microstructure. The D/E_{2g} ratio for polished GC and pyrolytic graphite edge (PG) was relatively constant, while that of basal HOPG and PG varied significantly due to defects. The spatial heterogeneity of Rhodamine 6G Raman intensity following physisorption to carbon surfaces indicated that adsorption occurs at disordered regions, particularly defects on HOPG. This observation provides visual confirmation of previously reported correlations of defect area and physisorption. Chemisorption of dinitrophenylhydrazine was observed only at edge plane regions, confirming the localization of surface carbonyl groups on graphitic edge plane. Finally, chemisorption of nitroazobenzene radical formed from a diazonium precursor occurred at both basal and edge regions, but more rapidly at edge sites. The higher concentrations observed at edges are attributable either to more rapid reduction of the diazonium precursor or to more rapid attack of the radical, compared to basal plane. The results represent the first spatially resolved Raman examination of physi- and chemisorption at the monolayer level on carbon surfaces.

A long-standing goal in the study of electrode kinetics is understanding the surface structural properties that control electron transfer reactivity, particularly for carbon surfaces.[1−4] The vast majority of past investigations of both surface structure and kinetics have involved relatively large areas of an electrode surface ($\sim mm^2$), with the implicit assumption that the surface properties do not vary greatly within the area being examined. If kinetic or structural heterogeneity were present within the observation area, a macroscopic probe technique would yield a spatially averaged response. Examples of such spatially averaged measurements include XPS, Raman spectroscopy, IR reflection/absorption spectroscopy, and conventional electrode kinetic measurements.

Several approaches have been developed to improve the spatial resolution of electrode surface probes and therefore to more directly observe electrode heterogeneity. Optical techniques based on fluorescence microscopy or electrogenerated chemiluminesence (ECL) provide structural and kinetic information with $\sim 1\ \mu$m resolution. Kuhr et al. chemisorbed fluorescent tags to functional groups on carbon fibers and then observed their locations with optical microscopy.[5−7] Engstrom et al. observed ECL at electrochemically active sites on heterogeneous surfaces such as graphite−Kel-F composites and highly ordered pyrolytic graphite (HOPG).[8−10] STM and AFM provide spatial resolution of a few angstroms and led to the development of scanning electrochemical microscopy (SECM).[11−13] SECM provides spatial resolution well below 1000 Å and is particularly valuable for studying kinetic heterogeneity. However, SECM, STM, and AFM provide relatively little information about molecular structure of the adsorbates.

The current work on spatially resolved Raman spectroscopy of carbon electrode surfaces was undertaken for primarily two reasons: First, carbon occurs in various forms, all of which can exhibit heterogeneity of surface structure and properties. For example, defects on HOPG have been shown to be more reactive toward adsorption and electron transfer than the undisturbed basal plane, leading to extreme variation in observed properties.[1,4] Second, Raman spectroscopy is structurally informative about both adsorbates and the carbon substrate and can be conducted with $\sim 1\ \mu$m spatial resolution. An example of Raman imaging applied to laser-damaged HOPG has appeared previously.[14]

The current work involves the application of Raman microspectroscopy to HOPG and glassy carbon (GC) surfaces, in order to characterize structural heterogeneity. Variations in the inherent carbon structure were observed as spatial heterogeneity of the D/E_{2g} band intensity ratio. Spectral monitoring of physisorbed Rhodamine 6G (R6G) was performed to correlate the distribution of R6G with carbon structure. Finally, the spatial distributions of

(1) McCreery, R. L. In *Electroanalytical Chemistry*; Bard, A. J., Ed.; Marcel Dekker: New York, 1991; Vol. 17, pp 221−374.
(2) Kinoshita, K. *Carbon*: *Electrochemical and Physicochemical Properties*; Wiley: New York, 1988.
(3) McCreery, R. L.; Cline, K. K.; McDermott, C. A.; McDermott, M. T. *Colloids Surf.* **1994**, *93*, 211.
(4) McCreery, R. L. In *Laboratory Techniques in Electroanalytical Chemistry*, 2nd ed.; Kissinger, P. T., Heineman, W. R., Eds.; Marcel Dekker: New York, 1996; Chapter 10.
(5) Pantano, P.; Kuhr, W.; *Anal. Chem.* **1993**, *65*, 617.
(6) Hopper, P.; Kuhr, W.; *Anal. Chem.* **1994**, *66*, 1996.
(7) Pantano, P.; Kuhr, W.; *Anal. Chem.* **1991**, *63*, 1413.
(8) Pharr, C.; Engstrom, R.; Klancke, J.; Unzelman, P. *Electroanalysis* **1990**, *2*, 217.
(9) Bowling, R.; McCreery, R. L.; Pharr, C.; Engstrom, R. *Anal. Chem.* **1989**, *61*, 2763.
(10) Pharr, C.; Engstrom, R.; Tople, R.; Bee, T.; Unzelman, P. *J. Electroanal. Chem.* **1990**, *278*, 119.
(11) Engstrom, R.; Small, B.; Katlan, L. *Anal. Chem.* **1992**, *64*, 241.
(12) Bard, A. J.; Fan, F.-R.; Pierce, D.; Unwin, P.; Wipf, D.; Zhou, F. *Science* **1991**, *254*, 68.
(13) Wipf, D.; Bard, A. J. *J. Electrochem. Soc.* **1991**, *138*, L4.
(14) Treado, P. J.; Govil, A.; Morris, M. D.; Sternitzke, K.; McCreery, R. L. *Appl. Spectrosc.* **1990**, *44*, 1270.

S0003-2700(97)00553-2 CCC: $14.00

chemisorbed nitroazobenzene (NAB) and dinitrophenylhydrazine (DNPH) were examined, in order to characterize chemisorption sites.

EXPERIMENTAL SECTION

All chemicals were reagent grade from Exciton (Dayton, OH) or J.T. Baker Inc., with the exception of 4-nitroazobenzene-4′-diazonium tetrafluoroborate, which was prepared as described previously.[15] Glassy carbon (GC-20 and GC-30) was obtained from Tokai Inc. HOPG and Ticonderoga (natural) graphite were gifts from Arthur Moore at Union Carbide, and pyrolytic graphite (PG) was purchased from the Advanced Ceramics division of Union Carbide (now Praxair, Inc.).

GC samples were polished conventionally with 1, 0.3, and 0.05 μm slurries of alumina in Nanopure water or were fractured in air as described previously.[16] The fractured surface usually contained both "mirror" and "misty" regions, but the surface examined here was always the "mirror" region. The HOPG samples were either mechanically cleaved by using a razor blade inserted parallel to the *a* axis or by using adhesive tape to peel away several layers and expose a fresh surface. The pyrolytic graphite samples were cleaved with a razor blade and either used with no further modification or polished in the same manner as the GC samples.

R6G was adsorbed on carbon surfaces using the method previously reported by Kagan and McCreery.[17] Chemical modification of carbonyl groups on the carbon surfaces was done using DNPH, as reported previously by Fryling et al.[18] In order to reduce photodecomposition and thermal decomposition of chemisorbed DNPH, the laser was rapidly dithered along a line on the surface with a computer-driven mirror. To further reduce thermal damage, DNPH-modified surfaces were placed in a Teflon cell (Figure 1) filled with Nanopure water. Spectra were acquired through a quartz window positioned on the cell.

The imaging Raman spectrometer was a Dilor "X−Y" system with a 2000 × 800 front-illuminated CCD detector maintained at −140 °C. In all cases, a holographic band reject filter preceded a single spectrograph with either a 1200 or 1800 line/mm grating and the laser wavelength was 514.5 nm. Sampling modes provided by the Dilor system and used here include the following: (1) stationary Raman microprobe, with 10×, 50× ,or 100× objective; (2) microprobe profile scan in which several spectra (∼20) were obtained with the microprobe along a preselected line; (3) line focus, in which a servo mirror oscillates the microprobe focus along a line which is subsequently imaged on the vertical axis of the CCD; and (4) *x*−*y* imaging, in which the sample is translated by a motorized stage simultaneously with the line focus of mode 3. In each case, complete spectra are obtained with a spectral resolution determined by the slit width and dispersion, but each mode provides different spatial information and resolution. All quantitative comments about Raman intensities are based on the peak area for the bands of interest, unless noted otherwise.

In most cases, the defects and nonhomogeneities observed on carbon surfaces were present on the sample as cleaved or polished. In a few cases, however, a defect was produced artificially on HOPG to increase the edge plane density. A razor blade was gently touched to the freshly cleaved surface to produce a "scratch" which was visible with the 10× microscope objective. The width of the scratch varied from 15 to 45 μm.

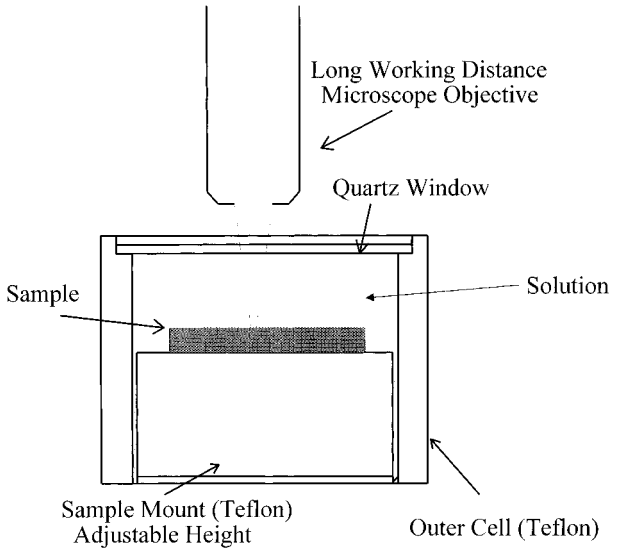

Figure 1. Diagram of Teflon sample cell and microprobe head. Laser light is focused by the microscope objective through a quartz window and onto the sample; scattered photons are collected by the same objective and passed through to the spectrograph entrance optics.

RESULTS AND DISCUSSION

The first issue considered was the inherent heterogeneity of the carbon surface itself. The Raman sampling depth is 100−300 Å,[19] so the Raman spectrum obtained with the microprobe is averaged over 1−3 μm in *X* and *Y* and ∼200 Å in depth. Microprobe spectra were obtained along a 125 μm line chosen at random on a given carbon surface. Representative spectra of six of the surfaces examined are shown in Figure 2. The ratio of the D band (∼1360 cm^{-1}) to E_{2g} band (∼1582 cm^{-1}) peak area was calculated from each spectrum, as well as the mean and standard deviation calculated for 15−50 spectra along the line. The results in Table 1 indicate the average D/E_{2g} ratio as well as its standard deviation over the surface. The Raman D/E_{2g} intensity ratio has been studied extensively as an indication of disorder in graphitic materials,[20−27] and its magnitude correlates inversely with the microcrystallite size determined from X-ray diffraction. The D band at ∼1360 cm^{-1} arises from breakdown of the **k**-vector selection rule from reduced symmetry at graphitic edges,[22,25] and the D/E_{2g} ratio increases with higher edge plane density.[27] Based on the original correlation of Tuinstra and Koenig,[21] the HOPG results in Table 1 indicate a crystallite size greater than 1000 Å, while the GC results indicate crystallites in the 10−50 Å range. Notice that polishing increases the D/E_{2g} band ratio on PG edges and GC and, in the case of PG, narrows the range of ratios observed.

(15) Liu, Y.-C.; McCreery, R. L. *Anal. Chem.* **1997**, *69*, 2091.
(16) Rice, R. J.; Pontikos, N.; McCreery, R. L. *J. Am. Chem. Soc.* **1990**, *112*, 4617.
(17) Kagan, M. R.; McCreery, R. L. *Langmuir* **1995**, *11*, 4041.
(18) Fryling, M. A.; Zhao, J.; McCreery, R. L. *Anal. Chem.* **1995**, *67*, 967.
(19) Alsmeyer, Y. W.; McCreery, R. L. *Anal. Chem.* **1991,** *63*, 1289. .
(20) Bowling, R.; Packard, R.; McCreery, R. L. *J. Am. Chem. Soc.* **1989**, *111*, 1217.
(21) Tuinstra, F.; Koenig, J. L. *J. Chem. Phys.* **1970**, *53*, 1126.
(22) Nemanich, R. J.; Lucovsky, G.; Solin, S. A. *Mater. Sci. Eng.* **1977**, *31*, 157.
(23) Vidano, R. P.; Fischbach, D. B.; Willis, L. J.; Loehr, T. M. *Solid State Commun.* **1981**, *39*, 341.
(24) Nakamizo, M.; Tamai, K. *Carbon* **1984**, *22*, 197.
(25) Lespade, P.; Al-Jishi, R.; Dresselhaus, M. S. *Carbon* **1982**, *20*, 427.
(26) Katagiri, G.; Ishida, H.; Ishitani, A. *Carbon* **1988**, *26*, 565.
(27) Wang, Y.; Alsmeyer, D. C.; McCreery, R. L. *Chem. Mater.* **1990**, *2*, 557.

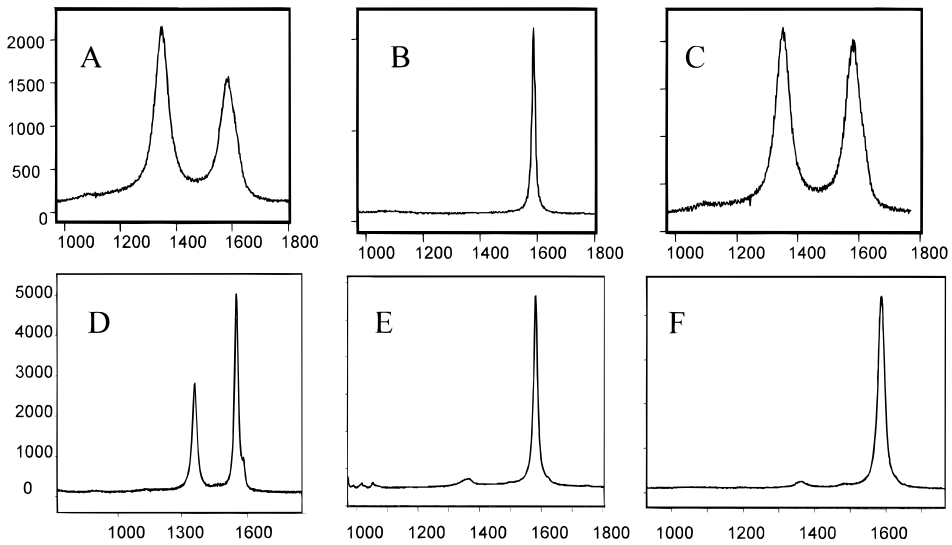

Figure 2. Raman spectra of carbon electrode materials collected with 50× long working distance objective: (A) polished GC-20; (B) basal plane HOPG; (C) fractured GC-20; (D) edge plane PG; (E) basal plane Ticonderoga; (F) basal plane PG.

Table 1

material	mean D/E_{2g} band area ratio	relative sd,%	no. of locations	D/E_{2g} min	D/E_{2g} max	av microcrystallite size,[a] Å
HOPG basal plane	0.0077 ± 0.0027[b]	35	50	0.0027	0.012	>1000
Ticonderoga, basal	0.064 ± 0.036	56	30	0.013	0.19	500
PG basal plane	0.175 ± 0.037	21	25	0.13	0.30	200
PG edge, fractured	0.223 ± 0.031	14	30			160
PG edge, polished	0.773 ± 0.04	5.2	25	0.721	0.826	50
GC, fractured	$1.65 \pm .064$	3.9	25	1.42	1.77	<50
GC, polished	1.84 ± 0.11	6.0	15	1.53	1.93	<50

[a] Estimated from mean D/E_{2g} ratio, according to ref 21. [b] Standard deviation, with the number of samples equaling the "no. of locations".

The surfaces listed in Table 1 fall into two general groups, based on the spatial variation of the D/E_{2g} ratio. GC and polished PG edge plane have low standard deviations (<10%) for the D/E_{2g} ratio, implying relatively homogeneous surfaces. The standard deviation of polished PG edge is significantly lower than the cut PG edge, presumably because polishing reduces crystallite size (as indicated by the increase in the D/E_{2g} ratio) and breaks up the larger crystallites. Therefore, GC (fractured and polished) and polished PG edge comprise a group with small crystallites which are homogeneously distributed. Of course, this homogeneity pertains to a minimum observation volume of about 2 μm × 2 μm × 200 Å, and heterogeneity within that volume would be spatially averaged during Raman observation.

The graphitic basal plane shows a lower value of the D/E_{2g} ratio but also larger spatial variation. The average D/E_{2g} ratio is in the order HOPG < Ticonderoga < PG basal < PG edge, as expected from literature values of crystallite size.[1] The high relative standard deviations of the basal surfaces indicate that these materials vary spatially, presumably due to defects of significant size compared to the ~2 μm spatial resolution of the microprobe. We have reported previously that defects on HOPG can result in significant variation in the observed adsorption and electron transfer behavior of HOPG basal plane.[28−30] The current results provide a spatially resolved spectroscopic probe of such defects, thus confirming STM results and adding structural information deduced from the Raman band intensities. The variations in D/E_{2g} ratio indicated by the relative standard deviation in Table 1 would not be apparent without a Raman microprobe, because conventional sampling would average over an area much larger than the defects.

Pits with diameters of 1−15 μm are commonly observed in microscopic images of polished GC,[31,32] and presumably result from gas bubbles remaining in the bulk material after fabrication. The structural and electrochemical properties of these pits are generally spatially averaged with the much larger flat regions, making any distinctive behavior difficult to observe. Figure 3 shows an optical micrograph of polished GC with spatially resolved spectra of the pit and flat regions within the pit. The D/E_{2g} ratio within a pit varied in the range of 0.25−0.5, much lower than the 1.6−1.8 on the flat plane. Figure 3B shows a Raman image of the same area as (A), with colors indicating the D/E_{2g} ratio. Red indicates a D/E_{2g} of 1.6−1.8, while blue is 0.25−0.5. The correspondence of the low D/E_{2g} ratio with the location of pits indicates that the pit walls are more ordered than either a fractured or polished GC surface. It is possible that the pits represent GC which is undisturbed by polishing or fracturing, and more representative of the bulk material. An alternative and probably

(28) McDermott, M. T.; Kneten, K.; McCreery, R. L. *J. Phys. Chem.* **1992**, *96*, 3124.
(29) Cline, K. K.; McDermott, M. T.; McCreery, R. L. *J. Phys. Chem.* **1994**, *98*, 5314.
(30) McDermott M. T.; McCreery, R. L. *Langmuir* **1994**, *10*, 4307.
(31) Kazee, B.; Kuwana, T. *Anal. Chem.* **1985**, *57*, 2736.
(32) Poon, M.; McCreery, R. L. *Anal. Chem.* **1986**, *58*, 2745.

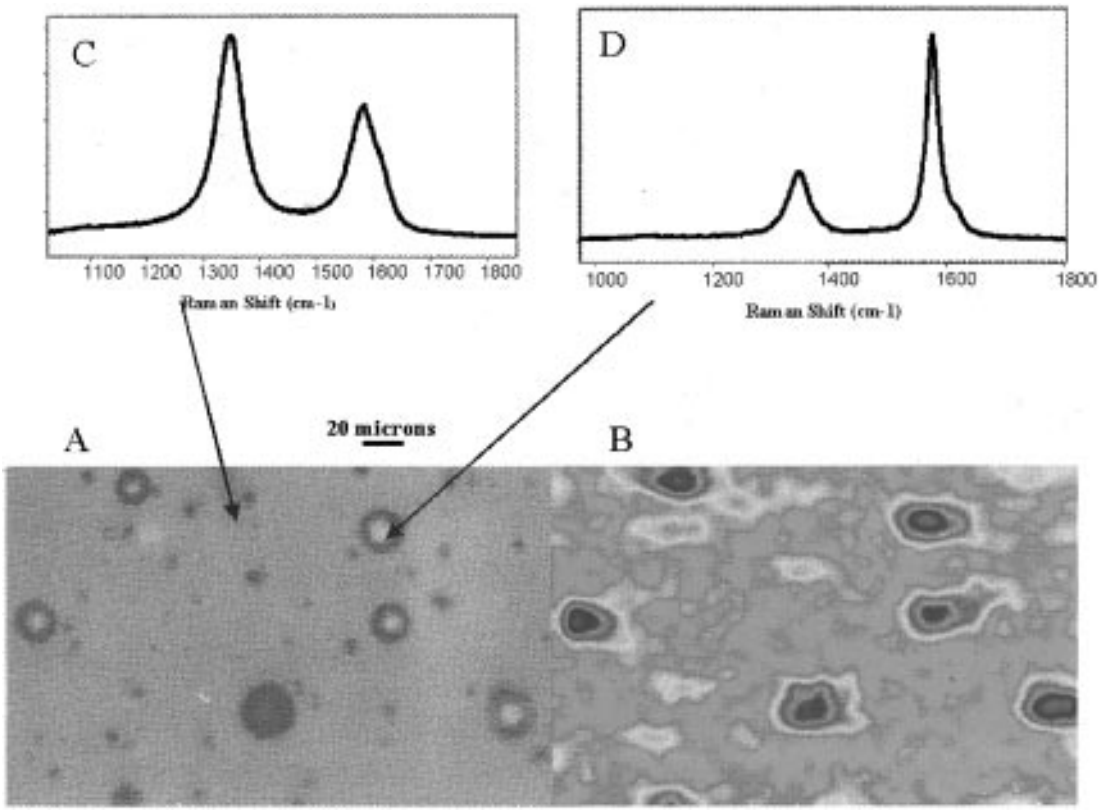

Figure 3. (A) Polished GC-20 100× bright-field image. (B) Raman image of same area as (A) constructed by taking the ratio of the 1360/1580 peak area from 1200 points inside the sample area. (C) Single spectrum acquired outside of pit. (D) Single spectrum acquired inside of pit.

more likely explanation is segregation and/or alignment of graphitic planes at the surfaces of bubbles during heat treatment.

Many reports have appeared on the relationship between Raman D/E_{2g} peak intensity ratio and carbon disorder,[1,2,20−27] and this disorder has been associated with adsorption and electrochemical reactivity.[3,4,9,30] The current results provide spatial information about carbon disorder, both location and heterogeneity. As noted elsewhere,[27] an increased D/E_{2g} ratio is more related to graphitic edges than to microcrystallites, although smaller microcrystallites naturally have a higher edge density. As will be shown next, these edge plane defects are essential for several types of physi- and chemisorption.

The remainder of the results deal with Raman observation of adsorbates on GC and basal HOPG surfaces. We have characterized these adsorbates previously with nonspatially resolved surface Raman spectroscopy and they were chosen for use here because of their large Raman cross sections and differing adsorption mechanisms.[15,17,18] R6G physisorbs on GC and exhibits a Langmuir isotherm.[17] Its native fluorescence is quenched by the carbon surface, and high signal to noise ratio Raman spectra may be observed for submonolayer coverage.[33] NAB is a nonselective chemisorber which forms a covalent bond with both edge and basal plane carbon atoms upon electrochemical reduction of a diazonium cation precursor.[15] DNPH forms a resonance Raman active surface species upon selective chemisorption to surface carbonyl groups.[18] The question addressed here is how these adsorbates are distributed on the carbon surfaces, and if there is any indication of preference for particular sites.

Since R6G adsorption to GC has been shown in a previous report[17] to form a monolayer governed by a Langmuir isotherm, it was studied first as a system expected to yield a spatially homogeneous distribution of adsorbate. After spontaneous adsorption of R6G from a 1 mM solution in methanol followed by a methanol rinse, Raman spectra were obtained over a 50×50 μm area that did not exhibit observable pits (spectra not shown). The ratio of the peak height of the 1180 cm^{-1} R6G band to that of the 1360 cm^{-1} GC band is proportional to average surface coverage within the 2×2 μm laser spot. For 64 spectra obtained within the 50×50 μm area, the 1180/1582 ratio averaged 0.129 with a relative standard deviation of 17%. The intensity of the 1180 cm^{-1} band showed no pronounced "hot" or "cold" spots on the image, indicating even distribution. Not surprisingly, physisorption onto a homogeneous GC surface (ignoring pits) is quite even, an observation consistent with Langmuir adsorption behavior. R6G Raman scattering within pits was not observable, apparently due to multilayer adsorption of trapped R6G, and accompanying fluorescence.

Raman observation of R6G distribution on HOPG basal plane led to quite different results. Initially, a razor blade was used to make an intentional defect on HOPG, shown in the micrograph of Figure 4A. The "trough" is ∼30 μm wide, which was large enough to permit removal of the sample from the microscope stage, adsorption of R6G, and then relocation of the same defect in the microprobe. In this manner, it was possible to obtain spatially resolved Raman spectra at a given defect before and after R6G adsorption. Figure 4C is the spectrum of the defect on HOPG before R6G adsorption, and (D) is the same spot after adsorption. The additional Raman features in (D) and in the difference spectrum (E) are due to R6G. For a line profile across the defect before adsorption, the 1360/1582 cm^{-1} ratio increases from ∼0.01 on basal plane to 0.05−0.2 within the defect. After adsorption,

(33) Kagan, M. R.; McCreery, R. L. *Anal. Chem.* **1994**, *66*, 4159.

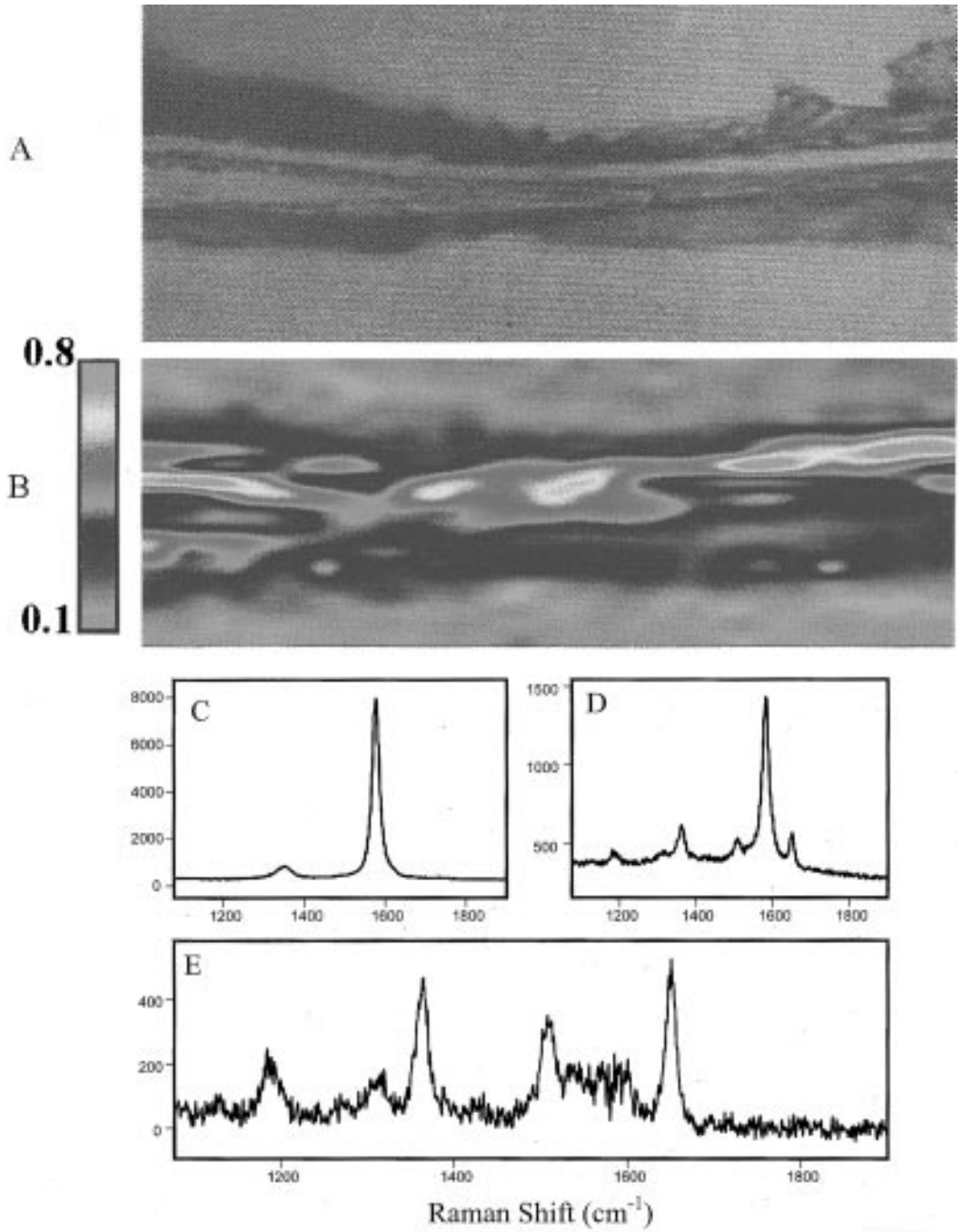

Figure 4. (A) 100× bright-field image of HOPG basal plane with an intentional defect. (B) Raman image of the same area as (A) after adsorption of R6G, constructed using the 1180/1580 peak area ratio from 1200 points. (C) Spectrum acquired near the intentional defect before R6G exposure. (D) Spectrum acquired near the intentional defect after exposure to R6G. (E) Resultant spectrum of (C) subtracted from (D).

the 1180/1582 cm^{-1} ratio increases from ~0.02 on basal plane to a range from ~0.1 to ~0.5 within the defect. Figure 4B shows a Raman image of the defect, with red indicating the highest 1180/1582 ratio, and lavender the lowest.

The possibility of observable R6G adsorption on apparently undisturbed basal plane was tested by obtaining spectra far away from any visual defects. Figure 5A is a spectrum of basal HOPG at least 300 μm away from any defects observable with a 50× microscope objective. Figure 5B is a spectrum of the same region after the sample is exposed to an R6G solution which would yield monolayer adsorption on GC. The difference spectrum (C) reveals no observable R6G bands, indicating an R6G coverage below the detection limit of ~0.05 monolayer. Therefore, Figures 4 and 5 support the conclusion that R6G preferentially adsorbs on defects and graphitic edge plane and interacts weakly with basal plane. It is possible that R6G *does* adsorb to basal plane and is thermally desorbed by the laser more quickly than at edge plane. Nevertheless, the adsorption on basal plane appears much weaker than on edge plane.

Figure 6 shows a similar measurement on a "natural" defect present on a cleaved HOPG surface. The defect was visible in the video micrograph, with a width of 2 μm and a length of >100 μm, but it did not exhibit an observable D band at ~1360 cm^{-1}. Following adsorption of R6G, there was observable Raman intensity from the adsorbate at the defect. So R6G adsorption was observed on an adventitious defect that was too small to yield an observable D band, meaning the D/E_{2g} ratio was less than 1% within the sampled area. It is likely that several layers of

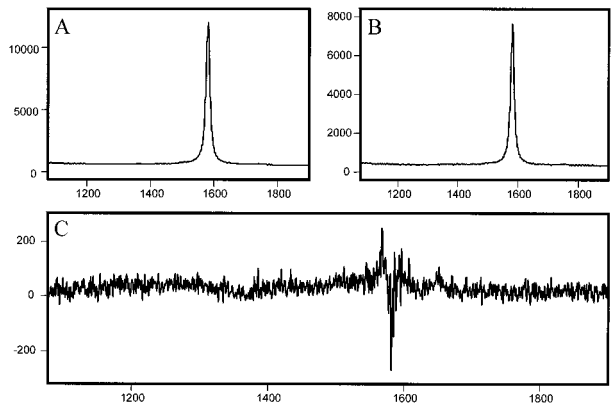

Figure 5. Raman spectra acquired with 50× long working distance objective of an HOPG basal plane surface with no defects visually apparent within 300 μm: (A) Spectrum of defect-free region before exposure to R6G. (B) Spectrum of defect-free region following exposure to R6G. (C) Resultant spectrum of (A) subtracted from (B).

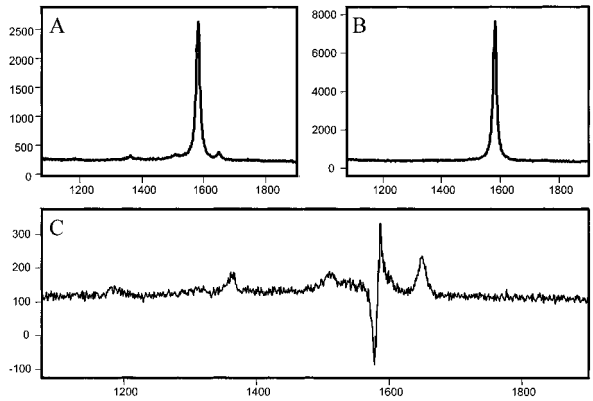

Figure 6. Raman spectra of an HOPG basal plane surface with a 2 μm adventitious defect acquired with 50× objective: (A) Spectrum of R6G adsorbed from solution. (B) Background spectrum before exposure to R6G. (C) Resultant spectrum of (B) subtracted from (A).

disordered graphite are necessary to yield observable 1360 cm^{-1} intensity, since the Raman sampling depth is greater than 30 graphite layers. Since adsorbed R6G is one monolayer (or less), the depth of the disorder does not affect its Raman signal. Apparently, the electronic disorder caused by the defect is sufficient for R6G adsorption under the conditions employed. Based on the 1180/1582 cm^{-1} peak intensity ratios, the amount of R6G adsorbed on this "natural" defect is less than half of that on the intentional defect of Figure 5.

The correspondence of the Raman and bright-field images in Figure 4 clearly supports the conclusion that R6G selectively physisorbs to defects on basal plane graphite. Local roughness is not sufficient to explain the greater Raman signal at defects.[17,34] While the conclusion of selective adsorption at defects is quite clear at the ~1 μm spatial resolution of the Raman microprobe, this is still a much larger scale than that observed with scanning probe techniques.[30] Such methods may detect basal plane adsorption below the Raman detection limit. Since there are a variety of chemical functional groups and sites present on edge plane defects, one might attribute the observed spatially selective adsorption to a specific interaction with some chemical site. However, we have observed strong monolayer adsorption on GC for neutral (β-carotene, bis(methylstyryl)benzene), cationic (R6G), and anionic (anthraquinonedisulfonate, AQDS) molecules[17,35] with a variety of structures. These observations imply a chemically nonspecific physisorption mechanism, which is promoted at edge plane defects, rather than a mechanism based on a specific chemical site. On the basis of STM and electrochemical results, we concluded previously that anthroquinonedisulfonate adsorption on HOPG depended on electronic disturbances present at edge plane defects.[30] Both the Raman and STM results support a nonspecific physisorption mechanism related to electronic changes in the HOPG basal plane at and near edge plane defects.

We reported previously that DNPH is a spectroscopic marker for surface carbonyl groups, since it forms a resonance Raman active adduct when the carbon surface is treated with DNPH reagent.[18] The DNPH reaction was used here to identify the location of surface carbonyl groups relative to defects on PG and HOPG surfaces. The ratio of a chemisorbed DNPH band (1142 cm^{-1}) to the 1582 E_{2g} band intensities is proportional to the C═O density. Conventionally polished GC surfaces were found to have 1−5% coverage of C═O groups, with an increase to ~10% with electrochemical oxidation.[18] Figure 7 shows Raman spectra of several carbon surfaces following DNPH treatment and after subtraction of the substrate spectrum. The signal to noise ratio is significantly lower than in previous reports, because of the reduced sensitivity of the microprobe. Basal plane HOPG shows negligible C═O coverage, as expected, while PG edge, GC, and an intentional defect all indicate the presence of surface C═O groups. The C═O coverage indicated by the 1142/1582 peak area ratio decreases in the order GC > HOPG defect > PG edge > HOPG basal plane. Surface carbonyls are believed to form spontaneously upon exposure of carbon to air, so a few percent coverage is expected on exposed edge plane regions. The spatial localization on defects demonstrated by Figure 7 confirms that carbonyl groups can form only on edges.

The chemisorbed aromatic species derived from the electrochemical reduction of diazonium ions comprise a third type of adsorber, in addition to R6G and DNPH. Saveant, et al. demonstrated that reduction of diazonium salts yields N_2 and a radical, which aggressively chemisorbs to both the edge and basal planes of graphite.[35,36] Monolayer coverage has been demonstrated on GC, and the chemisorbed aromatic molecule has been observed with Raman spectroscopy.[15,37] In the current work, we chose nitroazobenzene as the chemisorbed species, due to its high Raman cross section. 4-Nitroazobenzene-4′-diazonium was electrochemically reduced at various carbon surfaces and then the chemisorbed NAB was observed with Raman spectroscopy.

Spatially resolved Raman spectra of NAB chemisorbed on GC revealed even coverage, with minor variation in intensity similar to that observed for R6G. On HOPG, however, NAB coverage varied significantly near defects. Figure 8 shows spectra of HOPG on (A) and off (B) an intentional defect, following reduction of NAB diazonium cation for 75 s. If the time for electrochemical reduction of the NAB diazonium precursor was short (5 s), chemisorbed NAB was observed predominantly at edge plane defects. The area of the 1130 cm^{-1} band relative to the 1582 carbon band was 6.2 times higher on a defect than on visually perfect basal plane. When the diazonium reduction time was

(34) Kagan, M. R. Ph.D. Thesis, The Ohio State University, Columbus, OH, 1996.

(35) Allongue, P.; Delamar, M.; Desbat, B.; Fagebaume, O.; Hitmi, R.; Pinson, J.; Saveant, J.-M. *J. Am. Chem. Soc.* **1997**, *119*, 201.

(36) Delamar, M.; Hitmi, R.; Pinson, J.; Saveant, J. M. *J. Am. Chem. Soc.* **1992**, *114*, 5883.

(37) Liu, Y.-C.; McCreery, R. L. *J. Am. Chem. Soc.* **1995**, *67*, 3115.

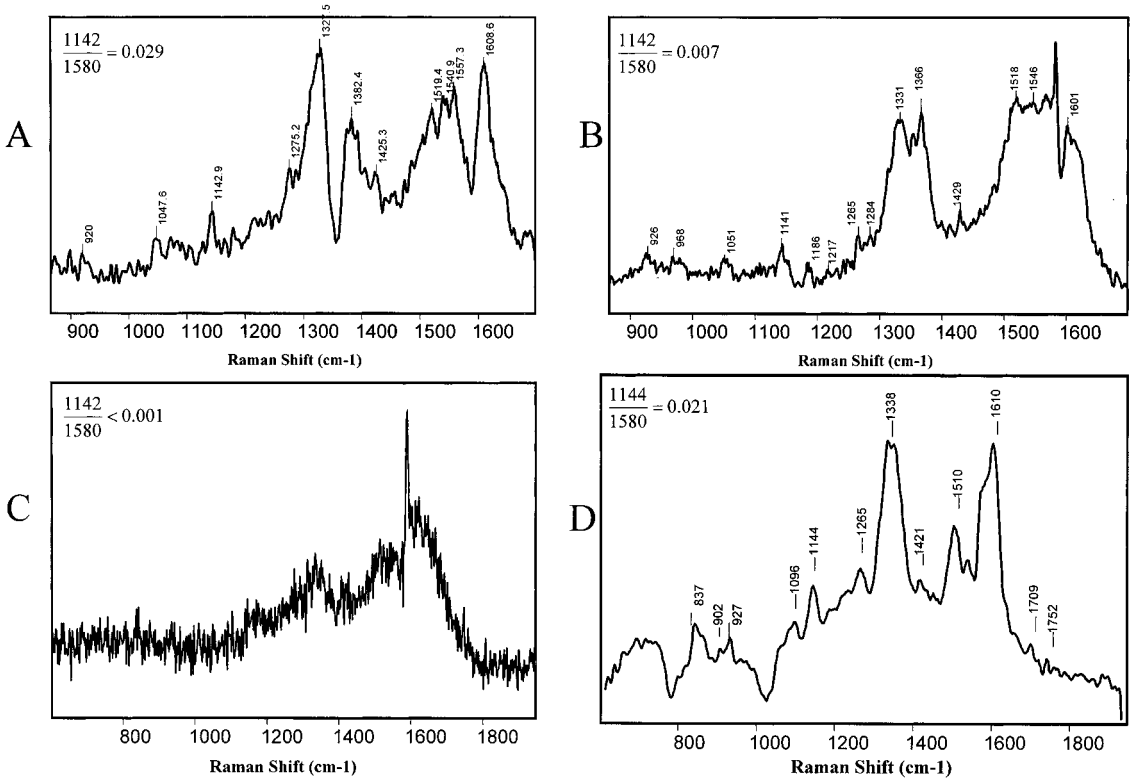

Figure 7. Raman spectra from various carbon surfaces after DNPH modification, acquired with 50× long working distance objective: (A) Polished GC-20. (B) PG edge plane. (C) HOPG basal plane. (D) HOPG basal plane at intentional defect. Substrate spectra were subtracted. Numerical inserts indicate band area ratios of the 1142 cm^{-1} DNPH peak to the 1582 carbon peak.

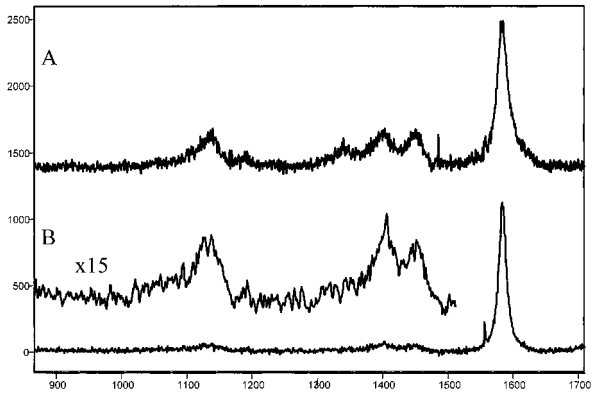

Figure 8. Raman spectra of HOPG basal plane surface after reduction of 0.4 mM NAB for 75 s acquired from the following: (A) intentional defect. (B) Visually defect-free surface at least 300 μm from intentional defect.

Table 2. Peak Ratios for Nitroazobenzene on HOPG

surface	reduction time, s	1130/1582 peak area ratio	defect to basal intensity ratio
defect	5	0.080	6.2
basal	5	0.013	
defect	15	0.170	4.7
basal	15	0.036	
defect	75	0.172	2.4
basal	75	0.073	

increased, NAB was observed on the basal plane, but still at lower intensity than at defects. Table 2 lists the intensities of NAB features relative to the 1582 E_{2g} band for three reduction times, both on and off a visible defect.

The diazonium reduction reaction used to chemisorb NAB was reported by Saveant et al. to produce monolayer coverage on both edge and basal surfaces, although the latter required a longer electrolysis time.[35] Figure 8 and Table 2 show that the chemisorbed NAB intensity is consistently higher on defects, more so for short electrolysis times. The stronger scattering on defects is not attributable to roughness, since the higher NAB number density is compensated by lower laser power density, resulting in comparable Raman scattering. For example, increasing the roughness of polished GC by a factor of 2.4 yielded only a 15% increase in scattering from physisorbed R6G.[17]

Another possibility for the greater NAB coverage at defects is preadsorption of diazonium reagent preceding electrolysis in the derivatizing solution. Based on the R6G results, we would expect NAB diazonium cation to preconcentrate on defects and be immediately reduced once a potential is applied. However, the diazonium concentration (0.4 mM) is high enough that diffusion can easily result in a monolayer quantity of NAB radicals at the surface in ~1 s. Even if preadsorption leads to a locally higher NAB concentration during derivatization, the electrolysis times in Table 2 are more than long enough to generate monolayer coverage if edge and basal graphite have equal reactivity. On a related point, there was no evidence that NAB derivatization was initiated at defects and then grew out into basal plane regions. Once the microprobe was located more than ~10 μm from a defect, the NAB coverage was spatially quite even, with no observable enrichment as defects were approached.

The most likely explanation for the results in Figure 8 and Table 2 is a significant difference in the rate of derivatization between edge and basal plane. Either electrochemical generation of the NAB radical or attack of the surface by the radical could be slower at basal plane than at edge plane. As the electrolysis time increases, the defects presumably saturate and the basal

derivatization continues, leading to a decrease in the ratio of defect to basal coverage with electrolysis time. Even for electrolysis times greater than 75 s, the defect coverage remained higher than the basal coverage, by a factor of ~2. The surface carbon structure should be different for basal vs edge bonding, and the maximum packing density of NAB may differ for this reason.

The consequences of these findings to previous conclusions about surface reactivity on carbon should be considered. Several authors attribute the low electron transfer reactivity of basal plane HOPG to its electronic properties, particularly its low density of electronic states (DOS) in the potential range of most redox systems.[4,38−40] The DOS is increased by disorder, due to the variety of energy levels created by defects, functional groups, etc. In the extremely disordered case of GC, the low DOS is absent and electron transfer rates to outer-sphere systems are comparable to those at metal.[41] Although the physical basis of physisorption may differ from that of electron transfer, they both depend on disorder. The nonspecific increase in physisorption near defects is analogous to the nonspecific increase in electron transfer rates. For both the physisorbed molecules studied thus far (R6G, β-carotene, AQDS, etc.) and for outer-sphere redox systems (Ru $(NH_3)_6^{2+/3+}$, Ir $Cl_6^{2-/3-}$, etc.) the electronic properties of the surface (DOS and local dipoles) are both important and nonspecific. In contrast, DNPH chemisorption is directly dependent on a functional group which can only exist at defects. Similarly, inner sphere redox reactions depend on particular sites. For example, $Fe^{3+/2+}$ electron transfer is many times faster on a surface containing 1% coverage of C═O groups than on an oxide-free surface.[41] Spatially resolved Raman spectroscopy provides a means not only to distinguish disorder-induced electronic effects from chemically specific chemisorption but also to permit spatial resolution of the consequences of surface chemistry.

CONCLUSIONS

Compared to fluorescence microscopy or scanning probe microscopy, Raman microspectroscopy has the advantage of providing structural information about the adsorbate. Furthermore, Raman is sensitive to disorder in the carbon substrate and permits the correlation of adsorption with defects in the graphite substrate. The availability of substrate and adsorbate spectra from Raman microspectroscopy yielded several conclusions. First, graphite samples of different origin varied significantly in defect density and structural heterogeneity. Second, physisorption of R6G was localized on defects of HOPG, due to a nonspecific interaction with the edge plane region. Third, chemisorption of DNPH, which is chemically specific for surface carbonyl groups, was observed only at defects. Fourth, nonspecific chemisorption of NAB occurred at both defects and basal regions, but more rapidly at defects. Overall, the results provide spatially resolved spectroscopic observation of carbon substrate heterogeneity, plus spatial visualization of nonspecific physisorption and both specific and nonspecific chemisorption. The results also reinforce previous conclusions about the importance of edge plane defects to the surface reactivity of carbon materials.

Received for review May 30, 1997. Accepted August 17, 1997.[⊗]

AC9705531

[⊗] Abstract published in *Advance ACS Abstracts,* October 1, 1997.

(38) Morcos, I.; Yeager, E. *Electrochim. Acta* **1972**, *15*, 257.
(39) Gerischer, H.; McIntyre, R.; Scherson, D.; Storck, W. *J. Phys. Chem.* **1987,** *91*, 1930.
(40) Gerischer, H.; Heller, A. *J. Phys. Chem.* **1991**, *95*, 5261.
(41) Chen, P.; McCreery, R. L. *Anal. Chem.* **1996**, *68*, 3958.